

Nonlinear Atom Optics: Multi-wave mixing with matter waves

L. Deng*†, E.W. Hagley*, J. Wen*, M. Trippenbach*‡, Y. Band*‡, P.S. Julienne*,
J.E. Simsarian*, K. Helmerson*, S.L. Rolston*, and W.D. Phillips*

* Atomic Physics Division, National Institute of Standards and Technology, Gaithersburg,
Maryland, 20899 USA

† Department of Physics, Georgia Southern University, Statesboro, Georgia 30460, USA

‡ Department of Chemistry and Physics, Ben-Gurion University of the Negev,
Beer-sheva, 84105, Israel

The advent of the laser as an intense, coherent light source gave birth to nonlinear optics, which now plays an important role in many areas of science and technology. One of the first applications of nonlinear optics was the production of coherent light of a new frequency by multi-wave mixing^{1,2} of several optical fields in a nonlinear medium, one whose refractive index depends on the intensity of the field. With the experimental realization of Bose-Einstein condensation³ (many atoms in a single quantum state) and the matter-wave "laser"^{4,5} (atoms coherently extracted from a condensate), we now have an intense source of matter-waves analogous to the optical laser. This has led us to the threshold of a new field of physics: nonlinear atom optics.⁶ Here we report the first experiment in this new field: the observation of coherent four-wave mixing (4WM) in which three sodium matter waves mix to produce a fourth. We show the nonlinear dependence of the generated matter wave on the densities of the input waves, a clear signature of a 4WM process.

The analogy between nonlinear optics with lasers and nonlinear atom optics with Bose Einstein condensates (BECs) can be seen in the similarities between the equations that govern each system. For a condensate of interacting bosons, in a trapping potential V , the macroscopic wave function Ψ satisfies a nonlinear Schrödinger equation⁷,

$$i\hbar \frac{\partial \Psi}{\partial t} = \left(-\frac{\hbar^2}{2M} \nabla^2 + V + U_0 |\Psi|^2 \right) \Psi, \quad (1)$$

where M is the atomic mass, U_0 describes the strength of the atom-atom interaction ($U_0 > 0$ for sodium atoms), and $|\Psi|^2$ is proportional to atomic number density. The nonlinear term $U_0 |\Psi|^2 \Psi$ in Eq.(1) is similar to the 3rd-order term $\chi^{(3)} |E|^2 E$ in the wave equation for the electric field E describing optical 4WM (where the susceptibility $\chi^{(3)}$ depends on the nonlinear medium). We therefore expect 4WM with

coherent matter waves analogous to optical 4WM. In contrast to optical 4WM, the nonlinearity in matter wave 4WM comes from atom-atom interactions; there is no need for an additional nonlinear medium.

The first theoretical study of nonlinear atom optics was reported in 1993,⁶ and the idea of 4WM using condensates prepared in different electronic states to enhance the nonlinearity was discussed in 1995.⁸ A recent calculation⁹ showed that the nonlinearity associated with the interaction between ground state atoms is large enough to observe 4WM with wavepackets created from existing BECs. To produce matter-wave mixing we create three overlapping wavepackets with momenta \vec{P}_n ($n=1,2,3$) and observe the creation of the 4WM wavepacket \vec{P}_4 that satisfies energy, momentum and particle number conservation (Fig. 1).

In our experiment we use Bragg diffraction of atoms from a moving optical standing wave¹⁰ to create the necessary three wavepackets, starting from a BEC. Briefly, we first form a condensate of $\sim 2 \times 10^6$ sodium atoms in the $3S_{1/2}, F=1, m=-1$ state using a combination of laser cooling and rf-induced evaporative cooling in a TOP (time-orbiting-potential) trap¹¹, without a discernible non-condensed fraction. We then adiabatically expand the potential¹⁰ in 4 s by simultaneously reducing the magnetic field gradient and increasing the rotating bias field. This reduces the trap frequencies in the \hat{x} , \hat{y} and \hat{z} directions to 84, 59 and 42 Hz. The asymptotic rms momentum width of the released condensate after adiabatic expansion is measured to be $0.14(2)\hbar k$ (all uncertainties reported in this paper are one standard deviation combined statistical and systematic uncertainties). Because this is small compared to $\sqrt{2}\hbar k$, the smallest momentum imparted to the condensate with the Bragg diffraction, the wavepackets will spatially separate as the system evolves.

After adiabatic expansion, we switch off the trap, wait 600 μs so that the trapping magnetic fields decay away and then apply a sequence of two Bragg pulses. Each 30 μs pulse is composed of two linearly polarized laser beams detuned from the $3S_{1/2}, F=1 \rightarrow 3P_{3/2}, F'=2$ transition by $\Delta/2\pi = -2$ GHz to suppress spontaneous emission. This large detuning makes Bragg scattering of the optical waves by the atoms, which could lead to a spurious scattering of atoms into \vec{P}_4 , completely negligible. The frequency difference between the two laser beams of a single Bragg pulse is chosen to fulfill a first-order Bragg diffraction condition that changes the momentum state of the atoms without changing their internal state.¹⁰ The first Bragg pulse is composed of two mutually perpendicular laser

beams of frequencies ν_1 and $\nu_2 = \nu_1 - 50$ kHz, and wavevectors $\vec{k}_1 = k\hat{x}$ and $\vec{k}_2 = -k\hat{y}$ ($k = 2\pi/\lambda$, $\lambda = 589$ nm). The maximum intensity of each beam is ~ 10 mW/cm². The intensity was chosen so that roughly 1/3 of the condensate atoms acquire momentum $\vec{P}_2 = \hbar(\vec{k}_1 - \vec{k}_2) = \hbar k(\hat{x} + \hat{y})$. 20 μ s after the end of the first Bragg pulse (well before the wavepackets are separated) the second Bragg pulse is applied. This pulse is composed of two counter-propagating laser beams with frequencies ν_1 and $\nu_3 = \nu_1 - 100$ kHz, and wave vectors $\vec{k}_1 = k\hat{x}$ and $\vec{k}_3 = -k\hat{x}$. The intensities of these laser beams were chosen to cause half of the remaining atoms in the momentum state $\vec{P}_1 = 0$ to acquire a momentum $\vec{P}_3 = \hbar(\vec{k}_1 - \vec{k}_3) = 2\hbar k\hat{x}$ (atoms in \vec{P}_2 are not affected by this pulse because of the Doppler shift of the light). We chose this pulse sequence so that *only* $\vec{P}_2 = \hbar k(\hat{x} + \hat{y})$ and $\vec{P}_3 = 2\hbar k\hat{x}$ are produced from $\vec{P}_1 = 0$. Thus we create, nearly simultaneously, three overlapping wavepackets of the requisite momenta. Without the nonlinear term in Eq.(1), one would expect only to observe these three wavepackets after they have spatially separated. As the three initial wavepackets separate however, the nonlinear term will produce an additional wavepacket that satisfies the condition $\vec{P}_4 = \vec{P}_1 - \vec{P}_2 + \vec{P}_3 = \hbar k(\hat{x} - \hat{y})$, (Fig. 1a) as well as energy and particle number conservation.

We have performed a 2-D numerical simulation of 4WM using Eq.(1) and the technique of Ref. 9. The interaction energy (chemical potential) was chosen to be the same as it would be in 3-D with a scattering length of 2.8 nm. The simulation releases 10^6 atoms from a trap with $\nu_x = 84$ Hz and $\nu_y = 59$ Hz. After 600 μ s the condensate was projected into the three initial momentum states. Fig. 2a shows the atomic density 1.8 ms after this projection. The most important feature of Fig. 2a is the new wavepacket of atoms with momentum $\vec{P}_4 = \vec{P}_1 - \vec{P}_2 + \vec{P}_3$ generated by 4WM. The 4WM peak does not appear when the nonlinear term is not present.

Fig. 2b is a false-color image showing the results of the experiment. The atoms were imaged 6.1 ms after the second Bragg pulse by optically pumping the atoms to the $3S_{1/2}, F = 2$ state, and absorption-imaging³ on the $3S_{1/2}, F = 2 \rightarrow 3P_{3/2}, F' = 3$ transition. The 4WM wavepacket is clearly visible. For this image the numbers of atoms in each wavepacket were measured to be: $N_1 = 4.8(5) \times 10^5$, $N_2 = 5.3(5) \times 10^5$, $N_3 = 5.1(5) \times 10^5$ and $N_4 = 1.8(2) \times 10^5$, where the uncertainties are mainly due to uncertainties in background subtraction. The numbers of atoms in the three initial wavepackets N_1^0 , N_2^0 and N_3^0 can be deduced using particle number conservation: $N_1^0 = N_1 + N_4$, $N_2^0 = N_2 - N_4$, and

$N_3^0 = N_3 + N_4$. Defining the 4WM efficiency to be $\varepsilon = \frac{N_4}{N}$ where $N = \sum_{j=1}^3 N_j^0 = \sum_{j=1}^4 N_j$, we obtain a conversion efficiency of 10.6(13)%. This is the best we have observed, although under similar conditions we have also observed conversion efficiencies of only 6%. This difference suggests the influence of some uncontrolled experimental conditions, such as laser beam inhomogeneities, or non-zero average velocity of the released condensate. By comparison, the calculation of Fig. 2a gives an efficiency of 10%, albeit for only 10^6 atoms.

Equation (1) can be used to make a simple prediction about the expected non-linear dependence of the 4WM signal on the numbers of atoms in the initial wavepackets. Substituting $\Psi = \sum_{j=1}^4 \Psi_j$ (where Ψ_j correspond to the individual momentum components) into Eq.(1), we find the initial rate of growth of the 4WM amplitude, $\frac{\partial \Psi_4}{\partial t} \propto \Psi_1 \Psi_2^* \Psi_3$. We estimate the number of atoms in the fourth wave by multiplying this rate by a characteristic interaction time τ , proportional to the diameter of the condensate, squaring and integrating over space: $N_4 \propto n_1 n_2 n_3 V \tau^2$, where the density $n_j \propto N_j^0 / V$. In the Thomas-Fermi limit,⁷ the volume of the condensate $V \propto N^{3/5}$, and $\tau \propto N^{1/5}$. Hence we expect $N_4/N \propto (N_1^0 N_2^0 N_3^0) N^{-9/5}$, a dependence which is supported by the numerical calculations. This nonlinear behavior is clearly manifest in the initial linear growth seen in Fig. 3 where we vary the number of atoms in the original BEC and measure the number of atoms in the respective wavepackets. The data also shows saturation at high N , as does the corresponding theory, although the maximum theoretical efficiency is somewhat higher.

Let us consider again Fig. 1b. Here, the process is seen as degenerate 4WM (where the magnitudes of all momenta are equal) in a geometry equivalent to phase-conjugation in optics¹² and indeed \vec{P}'_4 is the momentum conjugate of \vec{P}'_2 . Thus this can also be considered as a demonstration of phase conjugation with matter waves. As in the case of optical phase conjugation the process would work regardless of the angle between \vec{P}'_1 and \vec{P}'_2 (90° in the present case). If one alters the first Bragg pulse by changing only the angle of \vec{k}_2 (and appropriately changing v_2) the magnitude and direction of \vec{P}'_2 in the lab frame are changed so that in the moving frame only the angle of \vec{P}'_2 is changed.

It should be emphasized that just as optical 4WM requires coherent light sources to coherently build up the generated wave, a condensate is also crucial for coherent generation of new matter waves. If

atoms are above the condensation temperature, the number density is necessarily low and the phase matching condition is different for each velocity class. Both dramatically diminish the 4WM conversion efficiency.

In spite of the strong analogy between atom and optical 4WM, there are fundamental differences. In optical 4WM, the energy-momentum dispersion relation is $E = \frac{c}{n(k)}\hbar k$, ($n(k)$ is the dispersive refractive index) whereas for massive particles (neglecting the matter-wave refractive index due to the atom-atom interaction energy) $E = \frac{P^2}{2M}$. Because we neither create nor destroy atoms, the only 4WM processes allowed for matter waves are particle number conserving. This is not the case for optical 4WM where, for example, in frequency tripling three photons are annihilated and one is created. Particle, energy and momentum conservation limit all matter 4WM processes to configurations that can be viewed as degenerate 4WM in an appropriate moving frame.

The present experiment used relatively large momenta. If we use momenta small enough to couple to phonons or other collective excitations of the condensate, we will be able to study these excitations and their non-linear interactions with each other and with large momentum excitations. We can also change the internal states by using Raman transitions⁵ to scatter atoms in one internal state from the matter-wave grating formed by atoms in a different internal state. It should even be possible to study 4WM between different isotopes or elements. Furthermore, just as nonlinear optics can create quantum correlations between photon beams, nonlinear atom optics may lead to the study of non-classical matter-wave fields.

References

1. Franken, P.A., Hill, A.E., Peters, C.W. & Weinreich, G. Generation of optical harmonics. *Phys. Rev. Lett.* **7**, 118-119 (1961).
2. Maker, P.D. & Terhune, R.W. Study of optical effects due to an induced polarization third order in the electric field strength. *Phys. Rev.* **137A**, A801-A818 (1965).
3. Anderson, M.H., *et al.* Observation of Bose-Einstein condensation in a dilute atomic vapor. *Science* **269**, 198-201 (1995).
4. Mewes, M.-O., *et al.* Output coupler for Bose-Einstein condensed atoms. *Phys. Rev. Lett.* **78**, 582-585 (1997).
5. Hagley, E.W. *et al.* A well collimated quasi-continuous atom laser. *Science* (in press).
6. Lens, G., Meystre, P. & Wright, E.W. Nonlinear Atom Optics. *Phys. Rev. Lett.* **71**, 3271-3274 (1993).
7. Dalfovo, F., Giorgini, S., Pitaevskii, L.P. & Stringari, S. Theory of trapped Bose-condensed gases. *Rev. Mod. Phys.* **71**, (1999).
8. Goldstein, E.V., Plättner, K. & Meystre, P. Atomic phase conjugation. *Quantum Semiclass. Opt.* **7**, 743-749 (1995).
9. Trippenbach, M., Band, Y.B. & Julienne, P.S. Four wave mixing in the scattering of Bose-Einstein condensates. *Optics Express* **3**, 530-537 (1998).
10. Kozuma, M. *et al.* Coherent splitting of Bose-Einstein condensed atoms with optically induced Bragg diffraction. *Phys. Rev. Lett.* **82**, 871-875 (1999).
11. Petrich, W., Anderson, M.H., Ensher, J.R. & Cornell, E.A. Stable, tightly confining magnetic trap for evaporative cooling of neutral atoms. *Phys. Rev. Lett.* **74**, 3352-3355 (1995).
12. Shen, Y.R. *The Principles of Nonlinear Optics*, 249-251 (John Wiley & Sons, New York, 1984).

Acknowledgments: We thank K. Burnett, C.W. Clark, M. Kozuma, and D.E. Pritchard for stimulating discussions on the subject. This work was supported in part by the Office of Naval Research and NASA.

Figure Captions

Figure 1a. Momentum conservation, $\vec{P}_4 = \vec{P}_1 - \vec{P}_2 + \vec{P}_3$, (equivalent to phase-matching in optical 4WM) in the laboratory frame. Energy conservation requires $\vec{P}_4^2 = \vec{P}_1^2 - \vec{P}_2^2 + \vec{P}_3^2$.

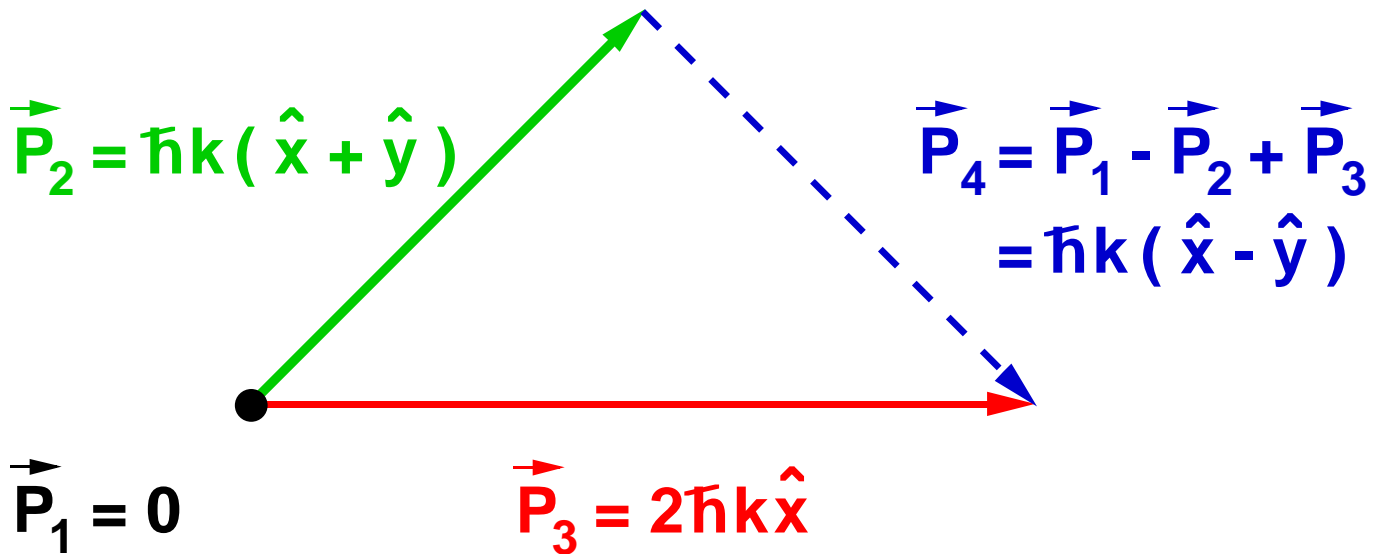
Figure 1b. It is always possible to view matter 4WM in a frame moving with velocity \vec{v} such that the three input momenta have the same magnitude, and two are counter-propagating. Then, in our case two atoms in momentum states $\vec{P}'_1 = -\hbar k \hat{x}$ and $\vec{P}'_3 = \hbar k \hat{x}$ are bosonically stimulated by wavepacket $\vec{P}'_2 = \hbar k \hat{y}$ to scatter into momentum states \vec{P}'_2 and $\vec{P}'_4 = -\vec{P}'_2 = -\hbar k \hat{y}$. Notice that the energy and momentum conditions are satisfied independent of the direction of \vec{P}'_2 . The 4WM wavepacket is a consequence of energy, momentum and particle number conservation when atoms are stimulated into the momentum state \vec{P}'_2 . Thus, 4WM can be viewed as the annihilation of momentum states \vec{P}'_1 and \vec{P}'_3 , and the creation of momentum states \vec{P}'_2 and \vec{P}'_4 (the minus signs in the energy and momentum conditions are attached to the state that gains atoms). It is this bosonic stimulation of scattering that mimics the stimulated emission of photons from an optical nonlinear medium. Alternatively, by choosing a frame of reference in which $\vec{P}'_1 = -\vec{P}''_2$ (or $\vec{P}''_2 = -\vec{P}''_3$), 4WM can also be viewed as matter-wave Bragg diffraction of \vec{P}''_3 (\vec{P}''_1) from the grating produced by the interference of two others.

Figure 2a. Calculated 2-D atomic distribution after 1.8 ms showing the 4WM. The calculations were performed only until the wavepackets completely separated due to constraints on the simulation grid-size. The momenta are those of Figure 1a. The field of view is 0.23 mm by 0.26 mm. Notice that atoms are removed primarily from the back-end of the wavepackets because these regions overlap for the longest time.

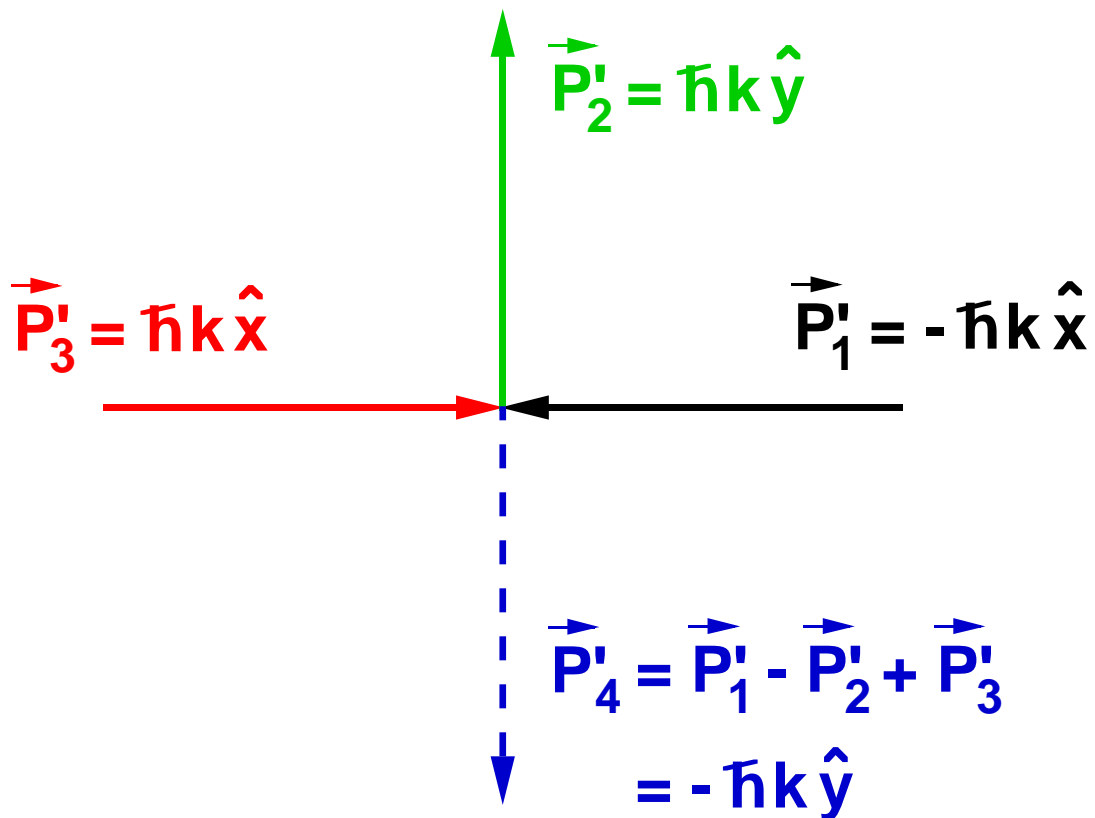
Figure 2b. A false-color image of the experimental atomic distribution showing the fourth (small) wavepacket generated by the 4WM process. The four wavepackets form a square measuring 0.26 mm by 0.26 mm, corresponding to the distance of 0.25 mm calculated using the experimental time of flight of 6.1 ms and the wavepacket momenta. We have verified that if we make initial wavepackets such that energy and momentum conservation cannot be simultaneously satisfied, no 4WM signal is observed. For instance, if we change the sign of the frequency difference between the two laser beams that comprise the second Bragg pulse, we will create a component with momentum $\vec{P}_3 = -2\hbar k \hat{x}$ instead of $\vec{P}_3 = 2\hbar k \hat{x}$. In this case there is no 4WM signal.

Figure 3. Efficiency $\frac{N_4}{N}$ as a function of $(N_1^0 N_2^0 N_3^0) N^{-9/5}$. The initial linear dependence is a signature of 4WM with matter waves. The dashed line is a fit to the first 12 points to guide the eye.

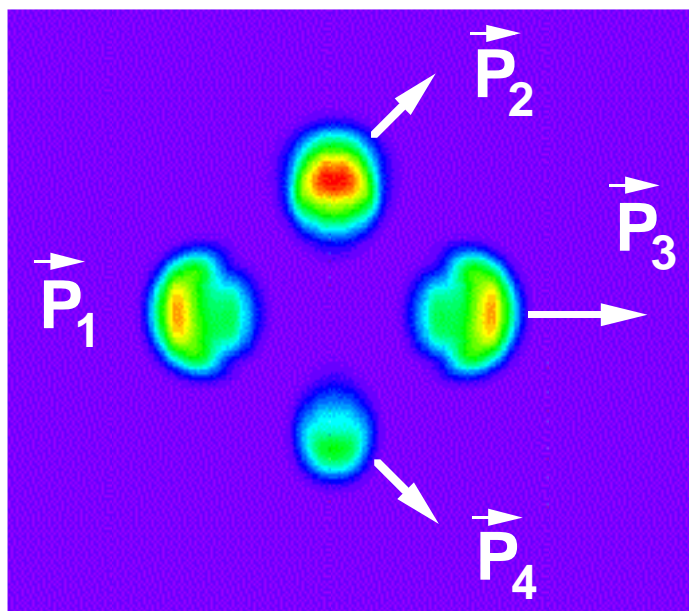
a. Lab frame:



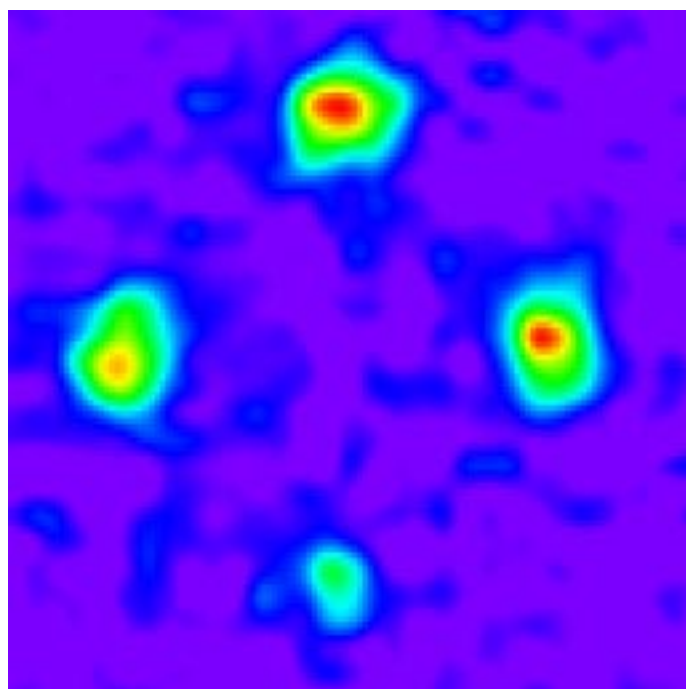
b. Moving frame: $\vec{v} = \frac{\hbar k}{M} \hat{x}$



a.



b.



← 0.57 mm →

